Available online at www.sciencedirect.com
ScienceDirect
Journal of Molecular Catalysis A: Chemical 258 (2006) 68–76
JOURNAL OF MOLECULAR CATALYSIS A: CHEMICAL
www.elsevier.com/locate/molcata

Photo-catalytic degradation of methyl orange and formaldehyde by $Ag/InVO_4$–TiO_2 thin films under visible-light irradiation

Lei Ge [a,b,*], Mingxia Xu [b], Haibo Fang [b]

[a] *Department of Materials Science and Engineering, China University of Petroleum, Beijing 102249, PR China*
[b] *School of Materials Science and Engineering, Key Laboratory for Advanced Ceramics and Machining Technology of Ministry of Education, Tianjin University, Tianjin 300072, PR China*

Received 18 February 2006; received in revised form 7 May 2006; accepted 9 May 2006
Available online 15 June 2006

Abstract

Novel $Ag/InVO_4$–TiO_2 composite thin films were synthesized via a sol–gel method in order to elucidate their visible-light-driven photo-catalytic performance. A wide range of techniques, such as X-ray diffraction (XRD), field emission scanning electron microscopy (FE-SEM), X-ray photo-electron spectroscopy (XPS), UV–vis absorption spectroscopy (UV–vis) and electron spin resonance (ESR) were applied to characterize the obtained composite thin films. The results revealed that the $Ag/InVO_4$–TiO_2 thin films extended the light absorption spectrum toward the visible region. Visible-light-induced photo-catalytic degradation of aqueous methyl orange (MO) and gaseous formaldehyde over Ag and $InVO_4$ co-doped TiO_2 thin films was observed. CO_2 and SO_4^{2-} were detected in the products of formaldehyde and methyl orange, respectively, indicating that formaldehyde and methyl orange were mineralized over the $Ag/InVO_4$–TiO_2 films under visible light. The effects of doped noble metal Ag by acting as electron traps and $InVO_4$ as a narrow band gap sensitizer in the $Ag/InVO_4$–TiO_2 films were also discussed. This study may provide an approach to treatment of organic pollutants by using visible light.

Keywords: Thin films; $Ag/InVO_4$–TiO_2; Visible light; Photo-catalytic activity

1. Introduction

Titanium dioxide has attracted great interest for its potential uses in catalysis [1], high selective adsorbents, photo-electrodes [2–4], photo-catalysts [5,6], gas sensors [7] and so on. Especially, the scientific interests in the photo-catalytic degradation of organic pollutants have grown quickly in the decade [8], TiO_2 has undoubtedly proven to be an excellent photo-catalyst for the oxidative decomposition of many organic compounds [9–11].

Although the process of UV irradiated TiO_2-photo-catalyzed degradation of organics proved to be a fascinating solution to this problem, the relatively wide band gap of 3.2 eV limits further applications of the material in the visible-light region ($\lambda > 400$ nm). For the efficient utilization of visible light, the development of visible-light-induced photo-catalysts for organics photo-degradation has become an urgent issue from the viewpoint of using solar energy. In order to endow the TiO_2 with higher photo-catalytic efficiency under visible-light illumination, numerous methods including transition metal or non-metal [12–15] doped TiO_2 and dye [16,17] or metal complex [18] sensitized TiO_2 have been developed.

Co-doped TiO_2 is also effective for enhancing the photo-catalytic activity. Li et al. [19] prepared the N–F-codoped TiO_2 photo-catalyst by spray pyrolysis method; they found that the N–F–TiO_2 photo-catalyst demonstrated the highest visible-light activity for the decompositions of both acetaldehyde and trichloroethylene, being much higher than that of N–TiO_2 and F–TiO_2. Hua et al. [20] synthesized the Pt and N co-doped TiO_2 nano-photo-catalyst, and found that the Pt/N–TiO_2 possessed high catalytic activity in the visible-light region. Wei et al. [21] prepared the La and N co-doped nano TiO_2 with high visible-light photo-activity. Alternative approach achieving visible-light photo-activity is to couple TiO_2 by using a narrow band gap semiconductor such as CdS [22,23], WO_x [24,25], Bi_2S3 [26], SnO_2 [27] and V_2O_5 [28], which have higher conduction band (CB) than TiO_2.

As a new type of semiconductor, $InVO_4$ has attracted interest for its special electrochemical and photo-catalytic proper-

* Corresponding author.
E-mail address: gelei08@eyou.com (L. Ge).

1381-1169/$ – see front matter © 2006 Elsevier B.V. All rights reserved.
doi:10.1016/j.molcata.2006.05.026

ties. Very recently, calculated by first principles calculations, and supported by experiments, $InVO_4$ has become a promising photo-catalyst with a narrow band gap ($E_g = 2.0$ eV), which is able to induce hydrolysis of water molecules under visible-light irradiation [29–31]. It would be desirable to estimate that the $InVO_4$–TiO_2 composite photo-catalyst may be excited by visible light and used as new visible-light-induced photo-catalysis. The noble metals such as Pt [32] and Au [33] deposited or doped on the TiO_2 have high Schottky barriers among the metals and thus act as electron trips, facilitating electron–hole separation and promoting interfacial electron transfer process [34]. Moreover, surface plasmon resonances of noble metal particles, which can be excited by visible light, increase the electric field around metal particles and thus enhance the surface electron excitation and electron–hole separation on noble metal-doped TiO_2 particles [35,36].

However, most of studies reported the powdered TiO_2 used as photo-catalyst under visible-light irradiation, the application of TiO_2 powder is limited since a post-treatment separation is required to recover the catalyst. Some works reported the doping of TiO_2 with nitrogen, such as the synthesis of $TiO_{2-x}N_x$ films by sputtering of TiO_2 precursor under a nitrogen/argon gas mixture [37,38]; however these methods need expensive equipments and complex procedures.

In this study, we report a new simple method for the preparation of Ag and $InVO_4$ co-doped TiO_2 photo-catalytic thin films by the sol–gel method. The $InVO_4$ samples were synthesized by the hydrothermal method at low temperature of 150 °C. The $InVO_4$–TiO_2 composite thin films were prepared on glass slide substrates with the aim of extending the light absorption spectrum toward the visible region. To promote electron–hole separation and efficiency of photo-catalytic reaction, the noble metal Ag from $AgNO_3$ solution was doped into the $InVO_4$–TiO_2 composite thin films. The Ag/TiO_2 and TiO_2 thin films were also prepared to be compared with the co-doped thin films. The photo-catalytic activity of the obtained thin films was evaluated by the photo-catalytic degradation of aqueous methyl orange and gaseous formaldehyde. To the best of our knowledge, this is the first report showing the preparation and visible-light photo-catalytic activity of Ag/$InVO_4$–TiO_2 films deposited on glass slide substrates via the sol–gel method. This work may provide new insights into the preparation of highly photo-active TiO_2 thin films under visible-light irradiation.

2. Experimental

2.1. Chemicals

Indium chloride ($InCl_3$) and ammonium metavanadate (NH_4VO_3) were used as precursors of indium vanadate ($InVO_4$). Titanyl sulfate ($TiOSO_4$) was chosen as a Ti precursor. Silver nitrate ($AgNO_3$) was used as a source of Ag dopant. Indium chloride ($InCl_3$), ammonium metavanadate (NH_4VO_3), titanyl sulfate ($TiOSO_4$), silver nitrate ($AgNO_3$), hydrogen peroxide (H_2O_2, 30%) and ammonia solution ($NH_3{\cdot}H_2O$, 3 mol/l) used in the experiment were all analytical reagent grade.

2.2. Synthesis of orthorhombic $InVO_4$

A typical synthesis of $InVO_4$ was conducted in the following way: $InCl_3$ and NH_4VO_3 were first dissolved with distilled water respectively, the as-prepared $InCl_3$ solution with a concentration of 0.5 ml/l was put into a beaker, and then was slowly added the 0.5 ml/l NH_4VO_3 solution until the mole ratio of In^{3+} to VO_3^- reached 1:1; continual magnetic stirring was required to keep the reactant mixed uniformly, the pH value of the solution being adjusted to about 7 with ammonia solution. After that, the obtained sol was placed in a 150 ml stainless steel autoclave; the temperature of hydrothermal reaction was 150 °C for 4 h (temperature was raised at a heating rate of 1°/min). The obtained white slurry was centrifuged and washed with distilled water for three to five times to remove the remaining Cl^- and NH_4^+. Finally the sample was dried in a drying cabinet at 60 °C.

2.3. Preparation of Ag/$InVO_4$–TiO_2 thin films

The method of Ag/$InVO_4$–TiO_2 sol preparation is as follows: a 0.1 mol/l refluxed PTA sol (RS) was prepared by adding 50 ml 30% H_2O_2 to 450 ml dispersed white precipitate [$Ti(OH)_4$], which was then refluxed at 100 °C for 6 h according to the literature [39]. The obtained RS sol was mixed with certain amount of an as-prepared $InVO_4$ sample and $AgNO_3$ solution to form the various doping amounts of Ag/$InVO_4$–TiO_2 sols.

Glass slides were used as substrates. Before the deposition, substrates were ultrasonically cleaned in dilute HNO_3, acetone and absolute ethanol for 30 min, respectively. Finally, they were thoroughly rinsed with distilled water. TiO_2 thin films were deposited on the substrates by a dip-coating process at room temperature. The substrates were immersed into the as-prepared Ag/$InVO_4$–TiO_2 sol for 10 min. Upon withdrawal from the sol, the substrates were dried under infrared light at 60 °C for 30 min. Afterward, the substrates were ultrasonically rinsed with water and then the dried films were calcined at 500 °C for 30 min in air. The layers on substrates could be thickened by means of consecutive dip-coating processes. In such cases, substrates were only ultrasonically rinsed with water and dried at the end of the whole deposition process. The TiO_2, Ag/TiO_2 and $InVO_4$–TiO_2 thin films were also prepared by following the same procedure.

2.4. Characterization

The crystal structure of the samples was investigated by using X-ray diffraction (Rigaka D/max 2500v/pc X-ray diffractometer) with Cu Kα radiation at a scan rate of $0.1^\circ\ 2\theta\ S^{-1}$. The accelerating voltage and the applied current were 40 kV and 40 mA, respectively. The crystallite size was calculated from X-ray line broadening by Scherrer equation: $D = 0.89\lambda/\beta\cos\theta$, where D is the crystal size in nm, λ is the Cu Kα wavelength (0.15406), β is the half-width of the peak in radians and θ is the corresponding diffraction angle. The morphology of the samples was detected by using a JEOL JSF-6700F field emission scanning microscopy (FE-SEM) with an accelerating voltage of 10 kV. X-ray photo-electron spectroscopy (XPS) measurements were done on a PHI Quantum 1600 XPS instrument with a monochro-

matic Mg Kα source; the analyses were based on the following peaks: C1s, O1s, Ti2p, In3d, V2p. The binding energy scale was calibrated with respect to C1s peak of hydrocarbon contamination of 284.6 eV. The electron spin resonance spectra (ESR) were measured using an EMX-6/1 spectrometer (Bruker Analytik GMBH, Germany) in air under visible light ($\lambda > 400$ nm) irradiation. A 150-W Xe lamp with a 400 nm cut filter was used as the visible-light source. The setting for the ESR spectrometer were center field, 323.66 mT; sweep width, 25 mT; microwave frequency, 9.075 GHz; power, 450 μW. The UV–vis spectroscopy of the Ag/$InVO_4$–TiO_2 thin films were recorded on a UV–vis spectrophotometer (Exact Science Apparatus Ltd. of Shanghai 7230G).

2.5. Photo-catalytic activity

The visible-light photo-catalytic activities of the as-prepared films were evaluated by decomposition of gaseous formaldehyde and methyl orange in an aqueous solution at ambient temperature. The photo-catalytic degradation of formaldehyde was carried out in a 300 ml self-made cylindrical iron vessel, which consisted of an inlet, an outlet, and a sample port. Two pieces of the films samples were tested in the vessel perpendicular to the light beam. The optical system for the photo-catalytic reaction was composed of a 15 W energy saving lamp and a cut-off filter ($\lambda > 400$ nm). The distance between the films and the light source was 10 cm, where the average light intensity was 30 mW cm^{-2}. The gaseous formaldehyde in the contaminated atmosphere was obtained by the vaporization of formaldehyde liquid using the predetermined flow rate controlled by mass flow controllers. The mixture was then forced to flow through the photo-reactor for 30 min. Then, the photo-reactor was sealed and the photo-catalytic reaction was started by turning on the lamp. Subsequently, the concentration of formaldehyde and the carbon dioxide (CO_2) in the photo-reactor, obtained from the sample port, was measured with a gas chromatograph (GC-4009A) equipped with a flame ionization detector and a stainless steel column (Porapak R).

Experiments on photo-catalytic degradation of aqueous methyl orange were as follows: two pieces of 25 mm × 75 mm glass plate coated with films were settled into a 30 ml methyl orange aqueous solution with a concentration of 10 mg/l (30.56 μmol/l) in a 100 ml cylindrical glass reactor. A 15 W energy saving lamp was used as a light source. A cut-off filter ($\lambda > 400$ nm) was placed under the lamp. One face of the TiO_2 thin films was irradiated along the normal direction. Prior to photo-catalytic reaction, the methyl orange aqueous solution with TiO_2 thin films was kept in a dark condition for 20 min to establish an adsorption–desorption equilibrium. The concentration of methyl orange was determined by UV–visible spectrometry. UV–vis absorption spectra of irradiated samples were measured every 3 h. The changes in concentrations of methyl orange were estimated from the changes in absorbance of the absorption maximum at 500 nm. The product of methyl orange degradation was determined by an ion chromatograph with a conductivity detector (Dionex, DX-100).

3. Results and discussion

3.1. XRD patterns analysis

XRD is used to investigate the phase structures of the samples. The XRD pattern of the as-prepared $InVO_4$ sample is shown in Fig. 1. The X-ray diffraction peaks in Fig. 1 are corresponding to the orthorhombic phase of $InVO_4$ (JCPDF 48-0898) [40], and no other peaks are observed, indicating that the $InVO_4$ sample prepared by the hydrothermal method has absolutely the orthorhombic phase. The peak at 32.9° was used to calculate the mean crystallite size. The crystal size of the $InVO_4$ sample is estimated at about 20 nm calculated by Scherer equation, which demonstrates that the $InVO_4$ sample consists of nanocrystals.

Fig. 2 presents the XRD patterns of the pure and doped TiO_2 samples. In Fig. 2, five distinctive TiO_2 peaks are found at 25.3°, 37.9°, 48.0°, 54.6° and 62.8°, corresponding to anatase (1 0 1), (1 0 3, 0 0 4 and 1 1 2), (2 0 0), (1 0 5 and 2 1 1), (2 0 4) crystal planes (JCPDS 21-1272) [41], respectively, which indicates that the TiO_2 sample exist in the form of anatase phase after calcined at 500 °C. No extra peaks except for the TiO_2 anatase are

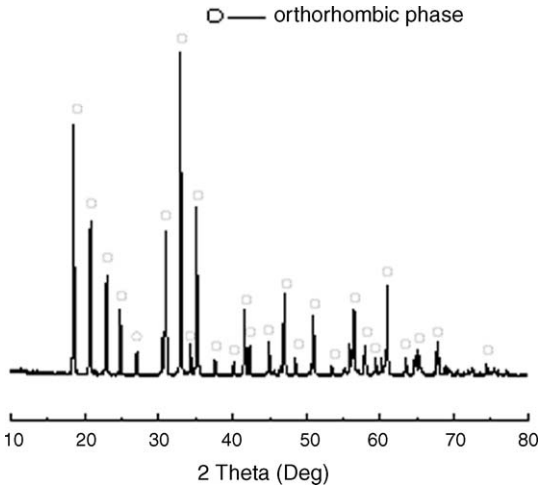

Fig. 1. XRD patterns of the $InVO_4$ samples prepared from hydrothermal method.

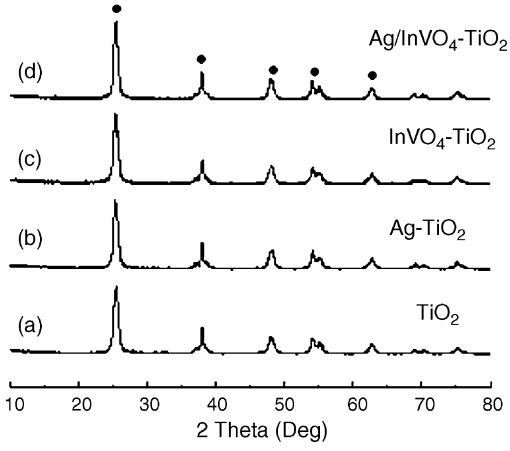

Fig. 2. XRD patterns of the TiO_2 samples: (a) pure TiO_2, (b) Ag–TiO_2, (c) $InVO_4$–TiO_2 and (d) Ag/$InVO_4$–TiO_2.

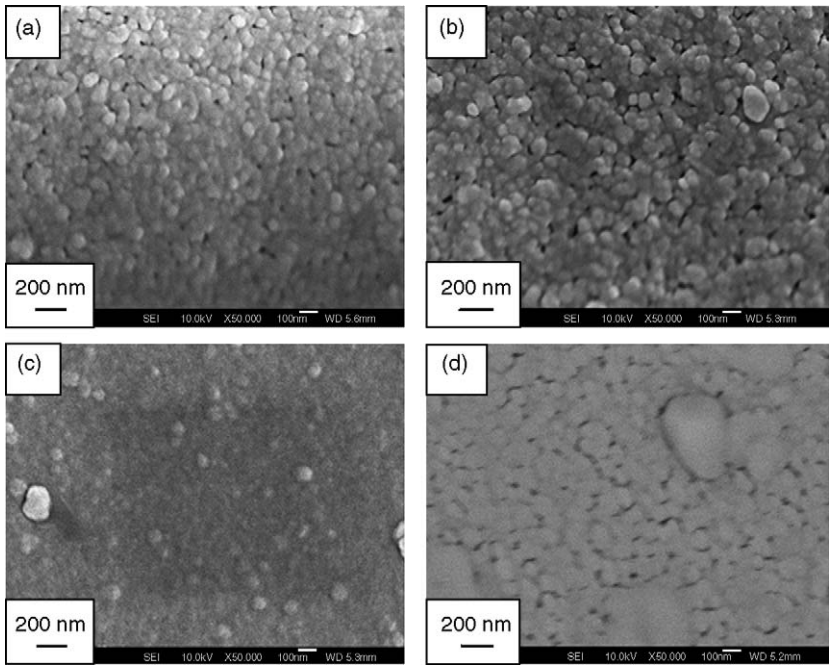

Fig. 3. FE-SEM micrographs of as-prepared samples: (a) TiO_2 thin film, (b) Ag–TiO_2 thin film, (c) $InVO_4$–TiO_2 thin film and (d) Ag/$lnVO_4$–TiO_2 thin film.

observed in Fig. 2. This may be due to the small amount of Ag and $InVO_4$ dopant (only 0.5 wt.%) and their high dispersion in samples.

3.2. FE-SEM micrographs of the films

Fig. 3 shows the FE-SEM micrographs of the as-prepared films. From Fig. 3a, the 500 °C heated pure TiO_2 films are compact and uniform, and no cracks and abnormal large particles are observed. The sphere particles of about 80–100 nm in diameters are found in the films, which can be attributed to the crystal growth and densification during the heating process at 500 °C. When TiO_2 films are doped with the noble metal Ag, the surface morphologies and roughness of the films are changed and become slightly heterogeneous; some large particles with diameters about 170–200 nm appear. The films become nonuniform after $InVO_4$ particles are added; some large particles obviously appear. The results of elemental analyses (EDX) showed that the film samples were uniform and homogeneous. It can be deduced that the large particles may be due to the agglomeration of nanoparticles in the films during the heat treatment When the film is co-doped with Ag and $InVO_4$, some extra large particles with diameters about 300–350 nm appear on the surface of the films, which can be due to the growth and densification of dopants during the treatment at 500 °C in air atmosphere.

The adhesion of the as-prepared films was evaluated by ultrasonic washing for 3 min and weight measurement. The results indicate that adhesion of the obtained films are good, no powders or fragments broke off from the films during ultrasonic treatment, and the weight of the films do not change after the ultrasonic process. To further investigate the adhesion, we scratched the films ten times using abrasive paper; no fragments broke off from the composite films, which demonstrated that the adhesion of the films was good enough to be used in the actual applications. The strong adhesion between the films and glass substrates may be attributed to the formation of the chemical bonds of Ti–O–Si at the interface of TiO_2 and substrates during the calcinations. Hence, the heat treatment not only enhanced the crystallization of TiO_2 thin films, but also improved the adhesion between the TiO_2 thin films and the glass substrates.

3.3. XPS studies

The X-ray photo-electron spectroscopy (XPS) was carried out to determine the chemical composition of the as-prepared Ag/$InVO_4$–TiO_2 thin films and the valence states of various species present therein. The XPS results show that the thin films deposited on glass substrates contain Ti, O, C, In, V and Ag elements. The photo-electron peak for Ti2p appears clearly at a binding energy of 458.8 eV, that for O1s at 530.6 eV, that for C1s at 284.6 eV, that for In at 444.6 eV, that for V at 515.8 eV and that for Ag at 367.7 eV. The peak positions are in agreement with the literature values [41,42]. The XPS peak for C1s is due to the adventitious hydrocarbon from the XPS instrument itself.

Fig. 4 shows high-resolution XPS spectra of the four elements of Ag (0.5 wt.%)/$InVO_4$ (0.5 wt.%)–TiO_2 thin films. The spin–orbit components (2p3/2 and 2p1/2) of Ti2p peak are well deconvoluted by two curves at approximate 458.8 and 465.2 eV, corresponding to Ti^{4+} in a tetragonal structure (Fig. 4a). Similarly, the O1s XPS spectrum (Fig. 4b) shows a narrow peak with a binding energy of 530.6 eV and slightly asymmetry. This peak was attributed to the Ti–O in TiO_2 and H_2O or OH groups on the surface of the sample. Although some H_2O is easily adsorbed on the surface of TiO_2 films during deposition process, the physically absorbed H_2O on TiO_2 is easily desorbed

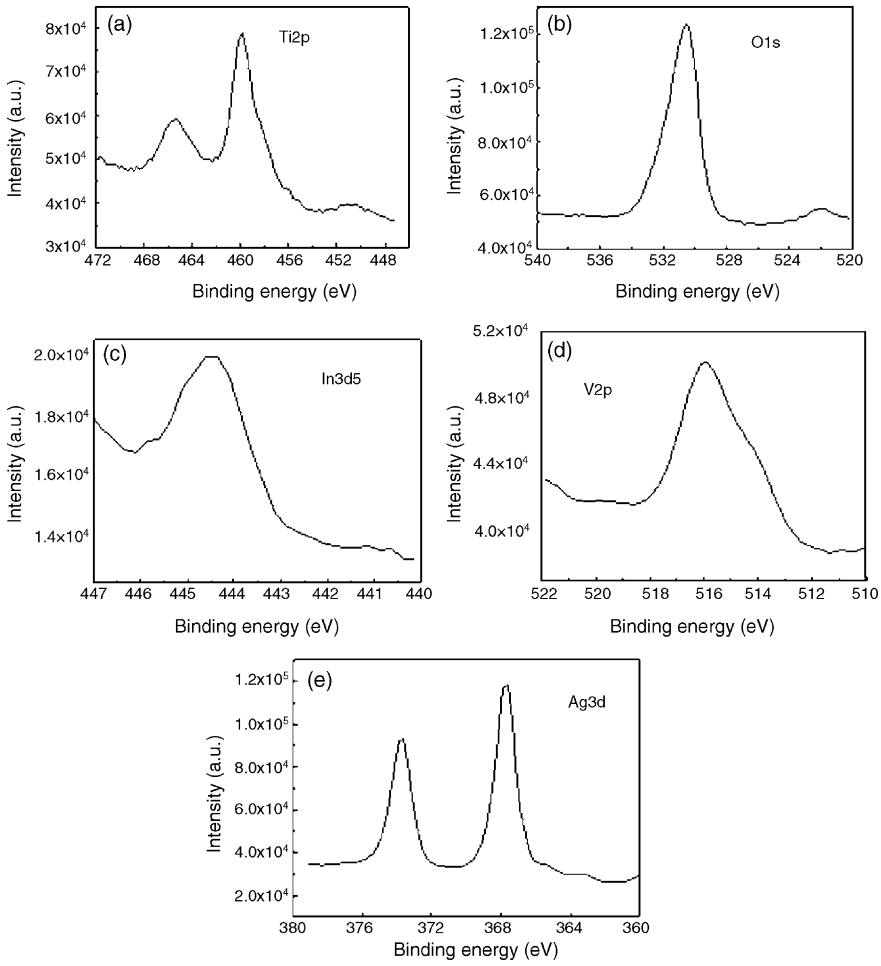

Fig. 4. High-resolution XPS spectra of the $InVO_4$–TiO_2 thin films: (a) titanium, (b) oxygen, (c) indium, (d) vanadium and (e) silver.

under the ultrahigh vacuum condition of the XPS system. Therefore, the hydroxyl on the surface can be attributed to the Ti–OH on the thin films. After heated at 500 °C, the TiO_2 thin films still contain a small amount of hydroxyl. This is probably due to the fact that the films easily adsorb water vapor in air, leading to the formation of hydroxyl on the films. The In3d5 peak is centered at 444.6 eV (Fig. 4c), which is different from the peaks at 444.08 and 445.24 eV assigned to crystalline indium oxide (In_2O_3) and amorphous indium oxide. Thus the In3d peak can be assigned to In^{3+} in $InVO_4$ [42]. The V2p peak is observed at 516.9 eV (Fig. 4d), corresponding to V^{5+} [42]. According to Ref. [29,30], the $InVO_4$ phase is stable when calcined at temperatures exceeding 800 °C. The heating temperature in our experiments is only 500 °C; therefore, the $InVO_4$ phase is not destroyed at low temperature of 500 °C. The XPS signals in 444.6 and 515.3 eV can be assigned to In^{3+} and V^{5+} in $InVO_4$ instead of In_2O_3 and V_2O_5. Fig. 4e shows the characteristic Ag3d peak that has a 6.0 eV splitting of the 3d doublet [34]. XPS peaks corresponding to Ag^+ ion are not found. This result confirms the presence of metallic silver doped in the TiO_2 films, which demonstrated that the Ag species does not react with $InVO_4$ in the Ag/$InVO_4$–TiO_2 thin films, the Ag species and $InVO_4$ relatively independently in enhance the photo-activity of TiO_2 films.

3.4. UV–vis absorption spectra

The thin films deposited on glass slides and calcined at 500 °C are transparent. The corresponding UV–vis absorption spectra for the as-prepared films are provided in Fig. 5. The UV–vis spectra of the pure TiO_2 films show strong absorption in UV

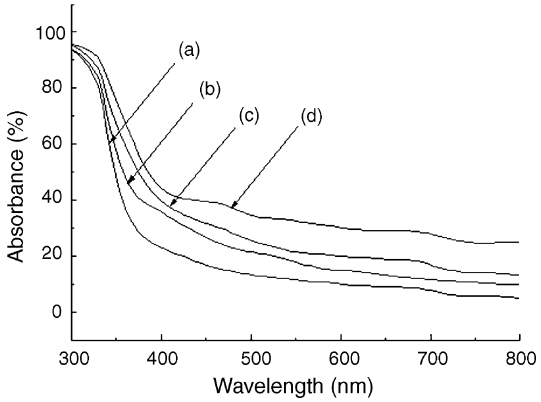

Fig. 5. UV–vis absorption of the film samples: (a) TiO_2 thin films, (b) Ag/TiO_2 thin films, (c) $InVO_4$–TiO_2 composite thin films and (d) Ag/$InVO_4$–TiO_2 thin films.

light region and little adsorption in visible-light region, while the other three film samples exhibit red-shift and absorption peaks in the visible-light region because of the existence of Ag and $InVO_4$ dopants in the films. The origin of the absorption of TiO_2 thin films in the visible-light region can be attributed to the glass substrates and surface defects in the pure TiO_2 thin films. The difference in absorption edge wavelength for the thin films clearly indicates the band gap of the various samples. To have a quantitative estimate of the band gap energies, the absorption onsets of the samples were determined by linear extrapolation from the infection point of the curve to the baseline. The absorption edge of the Ag/TiO_2 films is about 470 nm and the band gap is estimated to be 2.64 eV, while the edge of the absorption of the $InVO_4$–TiO_2 samples is shifted to approximately 560 nm, corresponding to a band gap energy of 2.21 eV. The co-doped Ag/$InVO_4$–TiO_2 thin films exhibit the largest visible-light absorption in the four samples, the absorption edge of the Ag/$InVO_4$–TiO_2 thin films has shifted to about 600 nm, corresponding to a band gap energy of 2.07 eV. The absorption onset for anatase TiO_2 thin films is 385 nm, with band gap energy of 3.22 eV. The results indicate that visible-light absorption of the TiO_2 films is enhanced by introducing Ag and $InVO_4$, and that the co-doped thin films show the best visible-light absorption and can be excited by visible light ($\lambda > 400$ nm).

3.5. ESR spectra

The ESR spectra of Ag and $InVO_4$ co-doped TiO_2 samples are shown in Fig. 6. Two signals A and B appeared under visible-light irradiation on the Ag/$InVO_4$–TiO_2 sample in the presence of oxygen. Signal A consists of a relatively sharp signal at $= 2.003 - 2.007$. The signal with $g_1 = 2.024$, $g_2 = 2.009$ and $g_3 = 2.003$ were unambiguously assigned to Ti^{4+}–$O_2^{\bullet-}$ adsorbed on the surface of anatase TiO_2 by some researchers [43,44]. Therefore, we assume that signal A is produced by $O_2^{\bullet-}$ radical signals on the Ag/$InVO_4$–TiO_2 samples. The signal B with g value of 1.991 can be assigned to the presence of Ti^{3+} on irradiated TiO_2 [45]. This strongly suggests an effective transfer of photo-generated electrons between Ag/$InVO_4$ and TiO_2.

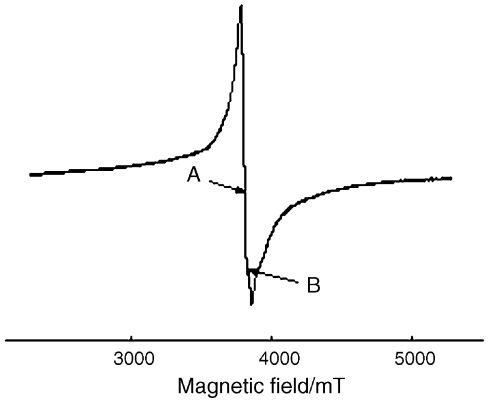

Fig. 6. ESR spectra of the Ag/$InVO_4$–TiO_2 sample after visible-light irradiating for 1 h.

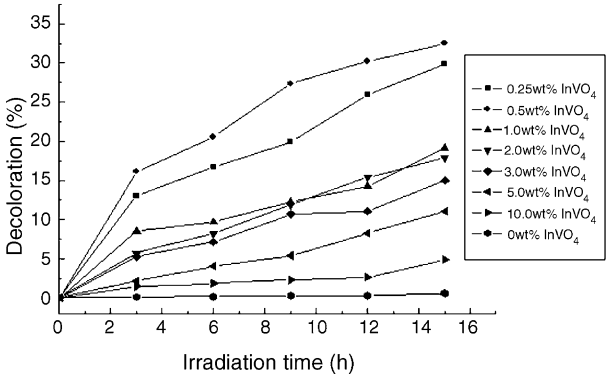

Fig. 7. Influence of $InVO_4$ doping amount on photo-catalytic degradation of methyl orange using $InVO_4$–TiO_2 composite thin films under visible-light irradiation.

3.6. Photo-catalytic activity of the films

The photo-catalytic activities of the film samples were evaluated by measuring the decoloration of methyl orange (MO) in aqueous solution under visible irradiation. Temporal changes in the concentration of MO were monitored by examining the variations in maximal absorption in UV–vis spectra at 500 nm. Fig. 7 shows the results of degradation of MO in the presence of the $InVO_4$ film samples. For comparison, the decoloration of pure TiO_2 thin films is given as well. When the lamp was turned on, the photo-degradation reaction of MO was initiated. The decoloration of MO solution increased with extending irradiation time. As shown in Fig. 4, decoloration of MO is not observed in the presence of pure TiO_2 thin films. However, in the presence of $InVO_4$–TiO_2 thin films, the decoloration of MO obviously increases. The difference in photo-catalytic activity for the samples deposited on glass slide substrates could be ascribed to the influence of $InVO_4$ dopant on the photo-catalytic activity of the TiO_2 thin films. Among the seven $InVO_4$–TiO_2 thin films with different $InVO_4$ doping, the 0.5 wt.% $InVO_4$–TiO_2 thin films exhibit the highest visible-light photo-catalytic activity, the decoloration rate of methyl orange solution reaching 32.5% after irradiated for 15 h. With increasing $InVO_4$ doping amount, the photo-activity of the samples obviously decreases, which may due to the reason that the $InVO_4$ nanoparticles agglomerate and do not well disperse when more $InVO_4$ was introduced into the films. The pure $InVO_4$ does not have photo-activity without NiO_x additive [29,30], and these factors have negative influence on the photo-activity of the films.

To further improve the visible-light photo-activity and investigate the influences of Ag doping on the $InVO_4$–TiO_2 thin films, Ag was doped into the $InVO_4$–TiO_2 thin films with the optimal $InVO_4$ dosage of 0.5 wt.%. The decoloration of the aqueous MO with Ag/$InVO_4$–TiO_2 thin films under visible-light irradiation is shown in Fig. 8. According to the XPS results, the Ag species exists in the form of metallic silver (Ag^0). Therefore, the role of Ag doping in the Ag/$InVO_4$–TiO_2 thin films is similar to the Ag/TiO_2 samples. Compared with the $InVO_4$–TiO_2 thin films, most of the Ag/$InVO_4$–TiO_2 thin films exhibit significant increase in the MO photo-decoloration rate. It is found that

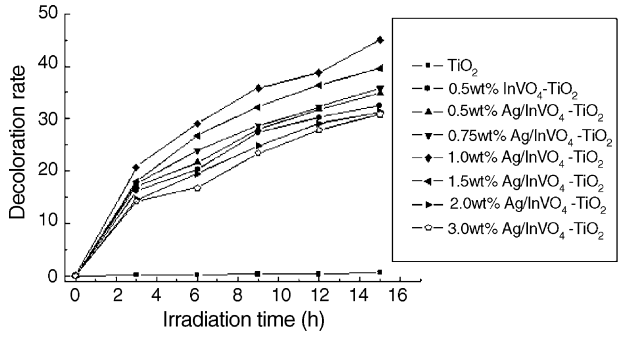

Fig. 8. Photo-catalytic degradation of methyl orange using $Ag/InVO_4$–TiO_2 thin films with different Ag doping amount under visible-light irradiation.

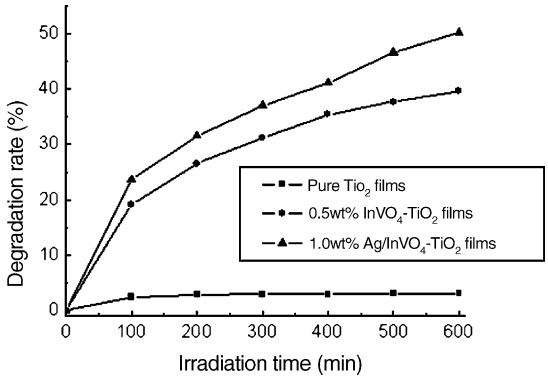

Fig. 9. Photo-catalytic degradation of formaldehyde on the surface of different film samples under visible-light irradiation.

the 1 wt.% Ag content is optimum to achieve the highest efficiency, and the composite thin films show a 12.5% increase in the MO photo-decoloration. More contents could be detrimental to the photo-decoloration efficiency; when the doped Ag content exceeds 1.5 wt.%, the decoloration efficiency of the co-doped film samples is below the $InVO_4$–TiO_2 thin films. It may be explained by assuming that at the Ag content below its optimum, the Ag particles doped in the films can act as electron–hole separation centers. The electron transfer from the TiO_2 conduction band to metallic silver particles at the interface is thermodynamically possible because the Femi level of TiO_2 is higher than that of silver metals [32]. This results in the formation of Schottky barrier at metal–semiconductor contact region, which enhances the photo-catalytic activity of the $InVO_4$–TiO_2 films. In contrast, at the Ag contents above its optimum, the Ag particles can also act as recombination centers. Thereby the probability for the holes capture is increased by the large number of negatively charged Ag particles on the films at high Ag contents, which reduces the efficiency of charge separation [32,36].

The anion of SO_4^{2-} is one of the main products of the MO degradation. Table 1 shows SO_4^{2-} concentration in the solution after photo-catalytic reaction. After the photo-catalytic reaction over pure TiO_2 thin films under visible-light irradiation, SO_4^{2-} ion concentration in the solution was null. It was obvious that MO was not decomposed but only somewhat adsorbed on the films. A SO_4^{2-} ion concentration of 4.9 μmol/l was detected in the solution after the photo-catalytic reaction over the 0.5 wt.% $InVO_4$–TiO_2 thin films under visible-light irradiation, which indicated that 16% of sulphur from MO was converted to sulphate. When the Ag was added into the $InVO_4$–TiO_2 samples, the concentration of SO_4^{2-} ion reached 8.3 μmol/l, indicating that 27.2% of the sulphur in MO was degraded. We could deduce that MO should have been decomposed to many fragments from the increase in SO_4^{2-} concentration after the photo-catalytic reaction.

It is well known that MO dye can absorb the visible light in the range of 400–600 nm, which is attributed to the ground state and excited state of the dye. Thus, the degradation of MO under visible-light irradiation should be the common effect of the MO and film samples, and therefore the observed visible response may not reflect the catalytic activity of the films. To resolve this problem, we performed another experiment on photo-catalytic degradation of gaseous formaldehyde under visible-light irradiation. Fig. 9 shows the result of the photo-degradation of gaseous formaldehyde on the film samples. The concentration of produced CO_2 is shown in Table 1. The photo-catalytic activities of doped thin films were much higher than those of the pure TiO_2 thin films. No CO_2 was detected in the phtotocatalytic products on TiO_2 thin films, indicating that the gaseous formaldehyde was only adsorbed on the surface of the TiO_2 films instead of photo-degradation. The degradation rate of formaldehyde on $InVO_4$–TiO_2 and $Ag/InVO_4$–TiO_2 thin films reached 39.6 and 50.3%, respectively, and the produced CO_2 was also observed as shown in Table 1. Therefore, the visible-light photocatalytic activity of the $InVO_4$–TiO_2 and $Ag/InVO_4$–TiO_2 thin films was confirmed in this study, the photo-catalytic activity of the $InVO_4$–TiO_2 sample was enhanced after doped with noble metal Ag.

Table 1
The Value of SO_4^{2-} and CO_2 concentration in the solution after methyl orange and formaldehyde degradation under visible-light irradiation

Film samples	TiO_2	0.5 wt.% $InVO_4$–TiO_2	1.0 wt.% $Ag/InVO_4$–TiO_2
SO_4^{2-} concentration (μmol/l)	0	4.9	8.3
CO_2 concentration (μl/l)	0	55.1	76.3

3.7. Photo-catalytic mechanism of the $Ag/InVO_4$–TiO_2 thin films

Using two semiconductors in contact having different redox energy levels of their corresponding conduction and valence bands can actually be considered as one of the most important promising methods for improving charge separations, increasing the lifetime of charge carriers, and enhancing the efficiency of the interfacial charge transfer to adsorbed substrate. For efficient interparticle electron transfer between the semiconductor that is considered as a sensitizer and TiO_2, the conduction band of TiO_2 must be anodic than the corresponding band of sensitizer. Under visible-light irradiation, only the sensitizer is excited, and electrons generated to their conduction band are injected into the inactivated TiO_2 conduction band. In our experiments,

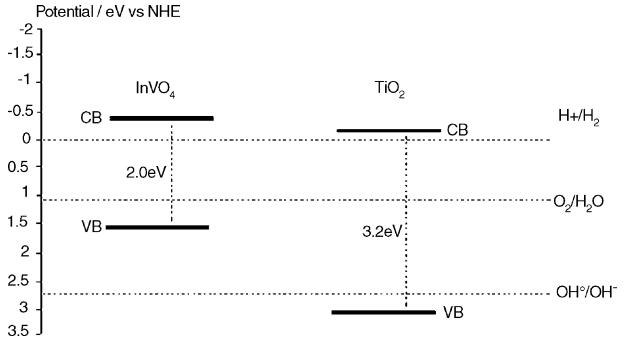

Fig. 10. Energetic diagrams of $InVO_4$ and TiO_2.

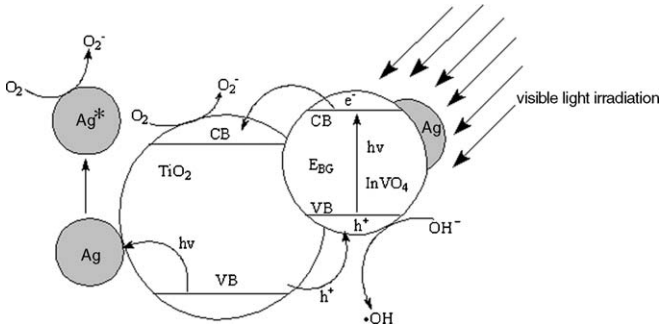

Fig. 11. Redox process of the valence and conduction bands of Ag/$InVO_4$–TiO_2 thin films samples under visible-light irradiation.

the methyl orange and formaldehyde can be photo-degraded by introducing $InVO_4$ nanoparticles into the TiO_2 thin films under visible-light irradiation. The ESR result indicates that the electrons from excited $InVO_4$ are injected into the conduction band of TiO_2 and then scavenged by molecular O_2 to yield the superoxide radical anion O_2^-. Based on the facts mentioned above, the interparticle electron transfer between $InVO_4$ and TiO_2 semiconductor system is deduced in this paper.

Fig. 10 depicts the valence and conduction bands for $InVO_4$ [29] and TiO_2 with their band gap energy. The conduction band of $InVO_4$ is more cathodic than that of TiO_2. In general, the difference in conduction bands between two semiconductors is the driving forces of electron injection. In the system of Ag/$InVO_4$–TiO_2, the $InVO_4$ can be excited and the excited electrons generate in the conduction band of $InVO_4$ and are quickly transferred to a TiO_2 particle from the $InVO_4$ particle under visible-light irradiation since the conduction band of $InVO_4$ is more negative than that of TiO_2 as shown in Fig. 10. The anatase TiO_2 is coupled by interparticle electron transfer from irradiated $InVO_4$ nanocrystals to its conduction band. The electrons are then scavenged by molecular oxygen O_2 to yield the superoxide radical anion O_2^-. Thus formed intermediates can interreact to produce hydroxyl radical ·OH. In addition, the holes remaining in the $InVO_4$ valence band after migration of excited electrons can also react with the hydroxyl groups (OH^-) to form $^\bullet$OH. It is well known that the $^\bullet$OH radical is a powerful oxidizing agent capable of degrading most pollutants. The transfer of charge should therefore enhance the photo-oxidiation of the adsorbed organic pollutants.

When the metallic Ag is doped into the films, the Ag particles can act as electron traps facilitating the electron–hole separation and subsequent transfer the trapped electron to the adsorbed O_2 acting as an electron acceptor [34] on the surface of the TiO_2 and $InVO_4$ as illustrated in Fig. 11. At the same time, more MO molecules are adsorbed on the surface of the composite thin films than on the TiO_2 samples, enhancing the photo-excited electron transfer from the visible-light sensitized MO to the conduction band of and subsequently increasing the electron transfer to the adsorbed O_2.

It has been reported that the surface plasmon resonance of some noble metals and complexes on TiO_2 is excited by visible light [43–46], enhancing the surface electron excitation and electron–hole separation, such as the Au–TiO_2 [36] and Pt–TiO_2 [35], the excitation of plasmon resonance may contribute to the enhancement in the photo-catalytic under visible-light irradiation, In this experiment, we deduced that the Ag dopant may play another role in enhancing the visible-light photo-activity of the Ag/$InVO_4$–TiO_2 composite thin films as shown in the left of Fig. 9. The acceptor surface state forms in the forbidden band of TiO_2 because of the Ag doping. The electron in the valence band of TiO_2 can be excited by visible light and migrate into the Ag particles, and then the doped Ag reach surface excitation state. The electrons on the surface of the excited Ag particles can react with molecular oxygen O_2 to produce the superoxide radical anion O_2^-. Thus formed intermediates can interact to produce hydroxyl radical $^\bullet$OH. Similarly, the holes remaining in the TiO_2 valence band after migration of excited electrons can also react with the hydroxyl groups (OH^-) in aqueous system and form the $^\bullet$OH with powerful oxidizing ability.

Based on the above explanation, Ag and $InVO_4$ in the composite thin films have a beneficial role in improving charge separation and extend TiO_2 in response to visible light. More studies may be carried out to obtain high visible-light active photo-catalyst in the near future based on this experiment.

4. Summary

Novel Ag/$InVO_4$–TiO_2 thin films with visible-light photo-activity were synthesized via a sol–gel method from the Ag and $InVO_4$ co-doped TiO_2 sol. The Ag/$InVO_4$–TiO_2 thin films extend the light absorption spectrum toward the visible region. XPS results reveal that doped Ag exists in the form of metallic silver. The ESR spectra have shown the evidence for the formation of superoxide radical anion ($O_2^{\bullet-}$) on the Ag/$InVO_4$–TiO_2 thin films under visible-light irradiation. The photo-catalytic experiments demonstrate that Ag doping can effectively enhance the photo-activities of $InVO_4$–TiO_2 thin films in the decomposition of aqueous methyl orange and gaseous formaldehyde under visible-light irradiation. CO_2 and SO_4^{2-} were detected in the products of formaldehyde and methyl orange, respectively, indicating that formaldehyde and methyl orange were mineralized over the Ag/$InVO_4$–TiO_2 films under visible light. It has been confirmed that Ag/$InVO_4$–TiO_2 thin films could be excited by visible light ($E < 3.2$ eV) due to the existence of the Ag and $InVO_4$ doped in the films. The photo-catalytic mechanism of Ag/$InVO_4$–TiO_2 thin films is also discussed in this paper.

Acknowledgement

This work was financially supported by the Doctor Foundation (Grant No. 20030056001).

References

[1] R.S. Sonawane, B.B. Kale, M.K. Dongare, Mater. Chem. Phys. 85 (2004) 52.
[2] C. Santato, M. Ulmann, J. Augustynski, Adv. Mater. 13 (2001) 511.
[3] L. Zhang, Y.F. Zhu, Y. He, W. Li, H.B. Sun, Appl. Catal. B 40 (2003) 287.
[4] J.C. Yu, X.C. Wang, X.Z. Fu, Chem. Mater. 16 (2004) 1523.
[5] H. Irie, Y. Watanabe, K. Hashimoto, J. Phys. Chem. B 107 (2003) 5483.
[6] O. Diwald, T.L. Thompson, T. Zubkov, J. Phys. Chem. B 108 (2004) 6004.
[7] B. Yuliarto, H.S. Zhou, T. Yamada, I. Honma, Y. Katsumura, M. Ichihara, Anal. Chem. 76 (2004) 6719.
[8] J. Tang, Z. Zou, J. Ye, Chem. Mater. 16 (2004) 1644.
[9] Y. Hu, C.W. Yuan, J. Cryst. Growth 274 (2005) 563.
[10] D.S. Muggli, L. Ding, M.J. Odland, Catal. Lett. 78 (2002) 23.
[11] W. Ma, J. Li, X. Tao, J. He, Y. Xu, J.C. Yu, J. Zhao, Angew. Chem. Int. Ed. 42 (2003) 129.
[12] T. Ihara, M. Miyoshi, Appl. Catal. B: Environ. 42 (2003) 403.
[13] R. Nakamura, T. Tanaka, Y. Nakato, J. Phys. Chem. B 108 (2004) 10617.
[14] C. Bura, Y. Lou, X. Chen, Nanoletter 3 (2003) 1049.
[15] S.U.M. Khan, M. Al-Shahry, W.B. Ingler, Science 297 (2002) 2243.
[16] G. Liu, J. Zhao, H. Hidka, J. Photochem. Photobiol. A: Chem. 133 (2000) 83.
[17] F. Zhang, J. Zhao, T. Shen, Appl. Catal. B: Environ. 15 (1998) 147.
[18] P.G. Hoertz, D.W. Thompson, L.A. Friedman, J. Am. Chem. Soc. 124 (2002) 9690.
[19] D. Li, N. Ohashi, S. Hishita, T. Kolodiazhnyi, H. Haneda, J. Solid State Chem. 178 (2005) 3293.
[20] N.P. Hua, Z.Y. Wu, Y.K. Du, Z.G. Zou, P. Yang, Acta Phys. Chim. Sin. 21 (2005) 1081.
[21] H.Y. Wei, Y.S. Wu, N. Lun, J. Mater. Sci. 39 (2004) 2100.
[22] L.M. Peter, D.J. Riley, E.J. Tull, K.G.U. Wijayantha, Chem. Commun. (2002) 1030.
[23] H.B. Yin, Y. Wada, T. Kitamura, T. Sakata, H. Hidaka, J. Photochem. Photobiol. A: Chem. 85 (1995) 247.
[24] J. Engweiler, J. Harf, A. Baiker, J. Catal. 159 (1996) 259.
[25] G. Ramis, G. Busca, C. Cristiani, L. Lietti, P. Forzatti, F. Bregani, Langmuir 8 (1992) 1744.
[26] Y. Bessekhouad, D. Robert, J.V. Weber, J. Photochem. Photobiol. A: Chem. 163 (2004) 569.
[27] K. Vinodgopal, P.V. Kamat, Environ. Sci. Technol. 29 (1995) 841.
[28] S.T. Martin, C.L. Morrison, M.R. Hoffmann, J. Phys. Chem.-US 98 (1994) 13695.
[29] Z. Zou, J. Ye, H. Arakawa, J. Mol. Catal. A: Chem. 168 (2001) 289.
[30] Z. Zou, H. Arakawa, J. Photochem. Photobiol. A: Chem. 158 (2003) 145.
[31] M. Oshikiri, M. Boero, J. Ye, F. Aryasetiawan, G. Kido, Thin Solid Films 445 (2003) 168.
[32] A. Sclafani, J.M. Herrmann, J. Photochem. Photobiol. A 113 (1998) 181.
[33] V. Subramanian, E. Wolf, P. Kamat, J. Phys. Chem. B 105 (2001) 11439.
[34] H.M. Sung-suh, J.R. C, H.J. Hah, S.M. Koo, Y.C. Ba, J. Photochem. Photobiol. A: Chem. 163 (2004) 37.
[35] Y. Cho, W. Choi, J. Photochem. Photobiol. A 148 (2002) 129.
[36] X.Z. Li, F.B. Li, Environ. Sci. Technol. 35 (2001) 2381.
[37] R. Silveryra, L.D.L. Torre, W.A. Flores, V.C. Martinez, A.A. Elguezabbal, Catal. Today 107–108 (2005) 602.
[38] T. Lindgren, J.M. Mwabora, E. Avendano, J. Phys. Chem. B 107 (2003) 5709.
[39] L. Ge, M.X. Xu, M. Sun, Mater. Lett. 60 (2006) 287.
[40] G.C. Xiao, D.Z. Li, X.Z. Fu, X.X. Wang, P. Liu, Chin. J. Inorg. Chem. 20 (2004) 195.
[41] L. Wu, Y. Jimmy, X.C. Wang, L.Z. Zhang, J.G. Yu, J. Solid State Chem. 178 (2005) 321.
[42] J.F. Moulder, W.F. Stickle, P.E. Sobol, K.D. Bomben, Perkin-Elmer Publishing Corp., MN, New York, 1992.
[43] T. Raji, A.E. Ostafin, O.I. Micic, D.M. Tided, M.C. Thurnauer, J. Phys. Chem. 100 (1996) 4538;
G. Zhao, H. Kozuka, T. Yoko, Thin Solid Films 277 (1996) 147.
[44] J.M. Coronado, A.J. Maira, J.C. Conesa, K.L. Yeung, V. Augugliaro, J. Soria, Langmuir 17 (2001) 5368;
J.M. Herrmann, H. Tahiri, Y. Ait-Ichou, G. Lassaletta, A.R. Gonzales-Elipe, A. Fernandez, Appl. Catal. B 13 (1997) 219.
[45] J.C. Yu, J. Lin, D. Lo, S.K. Lam, Langmuir 16 (2000) 7304;
L. Zang, C. Lange, I. Abraham, J. Phys. Chem. B 102 (1998) 10765.
[46] W. Zhao, W. Ma, J. Zhao, Chem. Eur. J. 9 (2003) 3292.